Type-II quasi phase matching in periodically intermixed semiconductor superlattice waveguides

David C. Hutchings,[1,*] Sean J. Wagner,[2] Barry M. Holmes,[1] Usman Younis,[1] Amr S. Helmy,[2] and J. Stewart Aitchison[2]

[1]Department of Electronics and Electrical Engineering, University of Glasgow, Glasgow, G12 8QQ, Scotland, UK
[2]Edward S. Rogers Sr. Department of Electrical and Computer Engineering, University of Toronto, 10 King's College Road, Toronto, Ontario M5S 3G4, Canada
*Corresponding author: D.Hutchings@elec.gla.ac.uk

Received October 22, 2009; revised March 12, 2010; accepted March 14, 2010; posted March 17, 2010 (Doc. ID 118655); published April 15, 2010

Second-harmonic generation using the type-II polarization configuration is demonstrated in quasi-phase-matched GaAs/AlGaAs superlattice waveguides. Phase-matching wavelengths and conversion efficiencies were determined for several quasi-phase-matching periods using 1.9 ps pulses. Saturation effects at high input power were concluded to be the result of third-order nonlinear effects. © 2010 Optical Society of America

OCIS codes: 190.5970, 190.4223.

Compound semiconductors are increasingly being exploited as nonlinear optical materials for optical frequency conversion and generation. Many semiconductors have nonlinear optical susceptibilities with values well in excess of conventional materials, such as lithium niobate. Semiconductors have an additional advantage that the transparency range extends further into the mid-IR than ferroelectrics and also encompasses the far-IR/terahertz range beyond the optical phonon resonance. Furthermore, growth and fabrication technologies are mature for GaAs- and InP-substrate wafers, allowing low-loss waveguide elements and, potentially, monolithic integration of laser diodes as on-chip pump sources.

The principal challenge in the adoption of semiconductors for optical frequency conversion and generation is achieving the necessary phase-matching condition, as there is no material birefringence in the zinc-blende (cubic) crystal structure to overcome the substantial dispersion. Consequently, quasi-phase-matching (QPM) technologies have attracted considerable interest. In particular, orientation-patterned growth (OPG) [1,2] has been successfully developed and is now commercially available in a bulk GaAs crystal format. However, the OPG method requires the QPM grating to be fixed at the wafer growth stage, and the subsequent mismatch in growth between alternate domains mean that low-loss waveguides and diode laser integration still remain as challenges.

An alternative method for semiconductors is domain-disordering QPM (DD-QPM), where the crystal structure is modified post-growth by quantum-well intermixing (QWI) to modulate the second-order susceptibilities. From initial demonstrations of type I second-harmonic generation (SHG) [3], improvements in the device fabrication have increased conversion efficiencies such that cw SHG has been recently demonstrated [4]. The type I geometry (corresponding to the $\chi^{(2)}_{zxy}$ tensor element) in zinc-blende semiconductor waveguides has the short wavelength in the TM polarized mode (perpendicular to the plane of a [001]-grown wafer). In anticipation of difference frequency generation or parametric generation with an integrated diode pump laser, the TE-polarized emission from the laser (in the plane of a [001]-grown wafer) would instead require a type II geometry (corresponding to the $\chi^{(2)}_{xyz}$ tensor element), where the short wavelength corresponds to a TE-polarized mode. In this Letter, it is demonstrated that DD-QPM semiconductor superlattices can exhibit optical frequency conversion in a type II geometry.

The waveguide structure used was the same as in previous studies [4] consisting of a 0.6-μm-thick core layer of 14:14 monolayer GaAs/$Al_{0.85}Ga_{0.15}As$ superlattice and cladding layers of bulk AlGaAs. DD-QPM gratings were formed by patterned QWI of the superlattice using ion implantation. A mask was formed by first using electron-beam lithography to write gratings in poly(methyl methacrylote) (PMMA). Written periods were 3.5–3.8 μm with nominal duty cycles of 0.4 and 0.5. A 2.3-μm-thick gold layer was then deposited by electroplating as an implantation mask. Inspection of the mask showed that the proportion of open areas was slightly reduced from the nominal value as written in PMMA. Ion implantation was carried out with 4.0 MeV As^{2+} ions at a dosage of 2.0×10^{13} cm^{-2} followed by rapid thermal annealing (RTA) at 775°C for 60 s. Lateral ion straggle results in implantation over a larger area than defined by the open mask, with QWI mediated by subsequent diffusion of the point defects under RTA. This leads to a $\chi^{(2)}$ modulation having a mark-to-space ratio modified from that defined by the original mask [5]. Photoluminescence measurements at 77 K showed a bandgap energy blueshift of 76 nm in the intermixed regions of the sample. Rib waveguides 3.0 μm wide and 1.0 μm deep were fabricated by reactive ion etching. The final sample was cleaved to a length of 0.6 mm. The range of QPM waveguides investigated here is shown in Table 1 and was somewhat limited by the yield of the overall fabrication process. Values for the optical losses at the fundamental wavelength were obtained from 3.5-mm-long waveguides (cleaved

0146-9592/10/081299-3/$15.00

Table 1. Linear Loss Coefficients and Conversion Efficiencies for Waveguides with Different QPM Periods and Duty Cycles

Period [μm]	Nominal Duty Cycle	TE Loss [cm^{-1}]	TM Loss [cm^{-1}]	Max. SH Conversion [%W^{-1} cm^{-2}]
3.5	0.4	0.9	1.3	350
3.6	0.5	1.2	1.8	220
3.7	0.5	1.0	2.0	280
3.8	0.5	0.7	1.2	200

from the same semiconductor chip) using the Fabry–Perot method with a narrow-linewidth, tunable laser source.

The waveguides were characterized using an optical parametric oscillator, producing optical pulses 1.9 ps long with a 2.4 nm spectral width, pumped by a mode-locked Ti:sapphire laser at a 75.6 MHz repetition rate. Light with a wavelength between 1550 nm and 1620 nm was end-fire coupled with a 40× objective into waveguide samples with average powers of up to 180 mW. A half-wave plate and a polarizing beam cube were used to set the input beam to a linear polarization 45° off horizontal. This launched both TE- and TM-polarized modes required for a type II interaction. Output light was collected with a 40× objective. The output fundamental wavelength and the generated second harmonic (SH) were separated using a long-pass filter. Output SH power was detected with a silicon photodetector, and the output spectrum was measured with an optical spectrum analyzer.

The variation of the fundamental wavelength corresponding to peak SHG with QPM period is shown in Fig. 1 for both type II and type I geometries. The slopes of these curves are similar, being dominated by the underlying material dispersion. For a particular fundamental wavelength the QPM grating period for phase-matching type II conversion is around 0.3 μm shorter than the period for phase-matching type I conversion in the same waveguide. This difference is commensurate with the measured dispersion

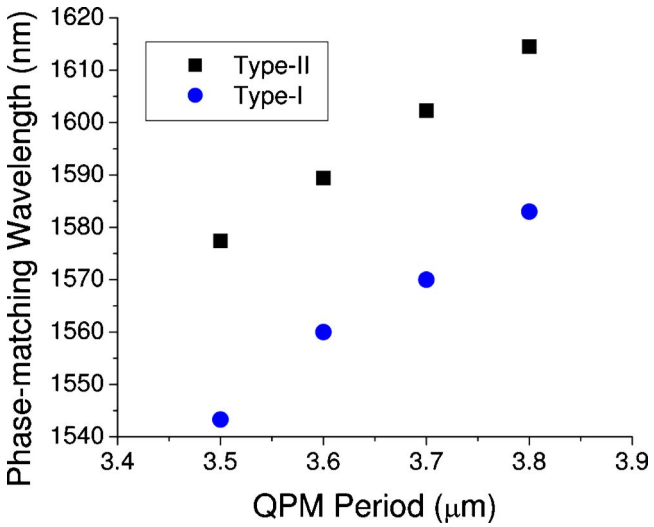

Fig. 1. (Color online) Dependence of phase-matching wavelength on QPM period for type I and type II phase matching.

and material birefringence in slab waveguides for similar superlattice wafers [6].

A pedestal of non-phase-matched SHG was observed over all wavelengths investigated. In addition to an increase of the SHG power when the phase-matching criteria for type II is satisfied, a narrowing of the SH pulse spectrum relative to the non-phase-matched case was observed on an optical spectrum analyzer. For example, with the 3.5 μm period the SH pulse spectral width was 0.96 nm when at a non-phase matched wavelength and 0.66 nm when at the phase-matching wavelength. This reflects a change from where the observed SH spectral width is limited by the bandwidth of the fundamental pulse spectrum to where the SH spectral width is limited by the phase-matching criterion. Furthermore, the relative proportion of SH in the TE-polarized mode is observed to increase on type II QPM resonance. In the following measurements, a polarizer was used after the filter such that the measured power values corresponds to the TE-polarized second harmonic only.

Input coupling efficiencies of the fundamental beam into the waveguides varied from one waveguide to the next. Thus, in order to account for these variations, we make use of the transmitted fundamental average powers when observing trends in the power dependence of the SHG process. However, the fundamental transmission decreased at high power levels, which indicates the presence of two- and three-photon absorption. As a result, output SH powers saturated at high input powers and deviated from the ideal quadratic dependence. Plotting the measured average SH power at the phase-matching wavelength as a function of the transmitted fundamental power as in Fig. 2 shows a near-quadratic power dependence of SHG at low power. However, the continued presence of the majority of the saturation in this plot indicates that the observed saturation cannot be completely accounted for by nonlinear losses, since these would affect the transmitted fundamental power as well. The observed saturation in this measure is attributed to self- and cross-phase-modulation of the fundamental modes owing to the known large nonlinear refraction in the vicinity of the half-bandgap [7,8]. Previous simulations of SHG in similar superlattice waveguides with third-order effects support this conclusion [9].

The SH conversion efficiency, defined as

$$\eta_{II} = \bar{P}_{2\omega}^{\mathrm{TE}}/(2\bar{P}_{\omega}^{\mathrm{TE}}\bar{P}_{\omega}^{\mathrm{TM}}L^2), \tag{1}$$

where $\bar{P}_{2\omega}^{\mathrm{TE}}$, $\bar{P}_{\omega}^{\mathrm{TE}}$, and $\bar{P}_{\omega}^{\mathrm{TM}}$ are average powers, is shown in Fig. 3 as a function of the center fundamen-

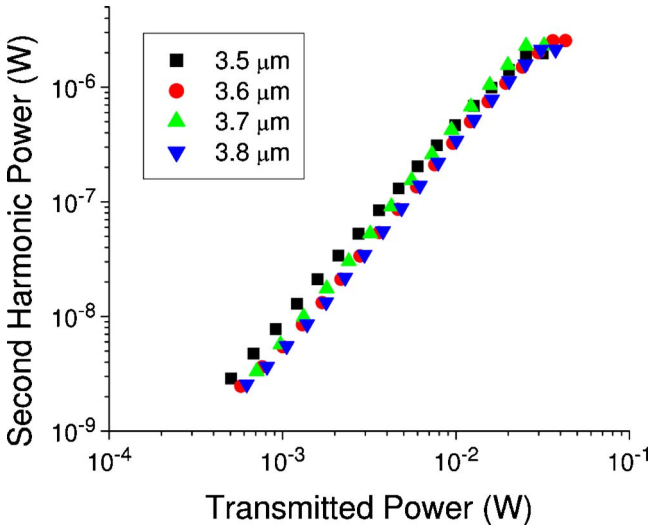

Fig. 2. (Color online) Output SH power as a function of transmitted fundamental power at the appropriate phase-matched wavelength for the QPM periods indicated.

tal wavelength for each of the waveguide samples. The transmitted fundamental power is restricted to the range 23–26 mW. The output optics and the rear facet reflectivity are accounted for so that the calculated conversion efficiencies correspond to inferred average optical power levels just before the rear facet. The maximum values for these conversion efficiencies are also obtained from a square power fit to the low power (<0.1 μW SH) data in Fig. 3 and are shown in Table 1. With the exception of the 3.6 μm period sample (where the results may be indicative of fabrication defects with correspondingly higher loss), a larger type II conversion efficiency was obtained at the shorter wavelength, which can be attributed to the expected larger modulation in the second-order susceptibility closer to the half-bandgap resonance.

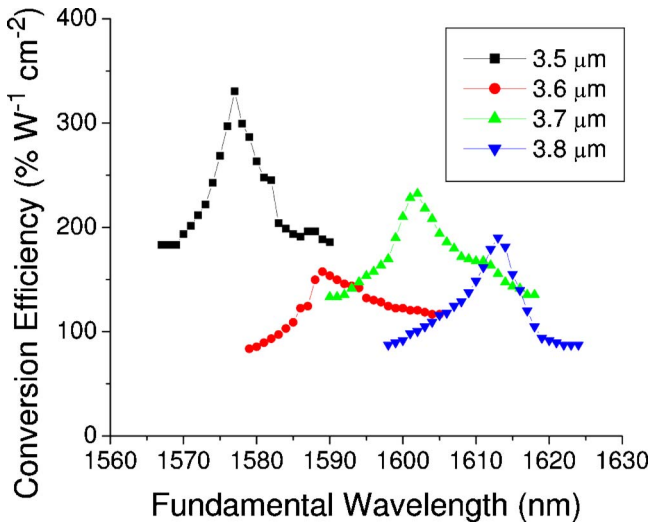

Fig. 3. (Color online) Wavelength dependence of the SH conversion efficiency (see text) for the different QPM periods.

For comparison, the equivalent type I low-power SH conversion

$$\eta_I = \bar{P}_{2\omega}^{\mathrm{TM}}/(\bar{P}_{\omega}^{\mathrm{TE}}L)^2 \qquad (2)$$

has a measured value of 1260 %W^{-1} cm^{-2} for a fundamental wavelength of 1570 nm. It is anticipated that the modulation obtained in the $\chi_{xyz}^{(2)}$ tensor element corresponding to type II conversion should be larger than the $\chi_{zxy}^{(2)}$ tensor element, corresponding to type I conversion at the same wavelength [10]. However, the lower conversion efficiency for type II could be the result of significantly larger SH optical losses for the TE polarization. For this waveguide structure, the TE mode at the SH wavelengths was found to have looser optical confinement relative to the TM mode owing to greater proximity to the cutoff condition.

In conclusion, type II SHG was demonstrated in domain-disordered QPM GaAs/AlGaAs superlattice waveguides. Conversion efficiency generally increased with shorter QPM periods and associated phase-matching wavelengths, which is in line with the predicted enhancement of $\chi^{(2)}$ near the half-bandgap energy. Saturation of the output SH powers at high input powers were attributed to higher-order nonlinear effects. While conversion efficiencies were lower than those of type I phase matching, this was likely the result of high losses for the TE-polarized SH mode. Overall, this demonstration of type II phase matching shows that optical frequency conversion in DD-QPM structures is compatible with monolithically integrated semiconductor diode pump lasers.

References

1. X. Yu, L. Scaccabarozzi, A. C. Lin, M. M. Fejer, and J. S. Harris, J. Cryst. Growth **301**, 163 (2007).
2. J. Ota, W. Narita, I. Ohta, T. Matsushita, and T. Kondo, Jpn. J. Appl. Phys. **48**, 04C110 (2009).
3. K. Zeaiter, D. C. Hutchings, R. M. Gwilliam, K. Moutzouris, S. V. Rao, and M. Ebrahimzadeh, Opt. Lett. **28**, 911 (2003).
4. S. J. Wagner, B. M. Holmes, U. Younis, A. S. Helmy, J. S. Aitchison, and D. C. Hutchings, Appl. Phys. Lett. **94**, 151107 (2009).
5. S. Charbonneau, E. Koteles, P. Poole, J. He, G. Aers, J. Haysom, M. Buchanan, Y. Feng, A. Delage, F. Yang, M. Davies, R. Goldberg, P. Piva, and I. Mitchell, IEEE J. Sel. Top. Quantum Electron **4**, 772 (1998).
6. T. Kleckner, A. Helmy, K. Zeaiter, D. C. Hutchings, and J. S. Aitchison, IEEE J. Quantum Electron. **42**, 280 (2006).
7. P. S. Kuo, K. L. Vodopyanov, M. M. Fejer, D. M. Simanovskii, X. Yu, J. S. Harris, D. Bliss, and D. Weyburne, Opt. Lett. **31**, 71 (2006).
8. S. J. Wagner, B. M. Holmes, U. Younis, A. S. Helmy, D. C. Hutchings, and J. S. Aitchison, IEEE Photon. Technol. Lett. **21**, 85 (2009).
9. S. J. Wagner, A. Al Mehairi, J. S. Aitchison, and A. S. Helmy, IEEE J. Quantum Electron. **44**, 424 (2008).
10. D. C. Hutchings, IEEE J. Sel. Top. Quantum Electron. **10**, 1124 (2004).